SAND--97-8556C

APPLICATION OF INTERNAL STATE VARIABLE PLASTICITY AND DAMAGE MODELS TO WELDING

CONF-970745--

J. J. Dike, A R. Ortega, D. J. Bammann, and J. F. Lathrop

Mechanics and Simulation of Manufacturing Processes Department
Sandia National Laboratories
P.O. Box 969
Livermore, CA 94551-0969

Abstract- An internal state variable constitutive model coupled with a ductile void growth model is applied in two finite element simulations of welding. Shrinkage of a 304 L stainless steel pipe due to multipass gas tungsten arc welds is presented as an example of tracking distortion far from the weld. Weld solidification cracking in Al-6061 disks is presented as an application of the plasticity model coupled with the damage model.

INTRODUCTION: Models of the two problems presented here require different degrees of detail due to the different aspects of mechanical response of interest. The first simulation presented is of a 3 pass GTA weld on 304 L stainless steel pipe. The pipe represented a cylindrical pressure vessel for which the reduction in volume capacity due to welding was of interest. Axial shrinkage of the pipe was used to characterize the reduction in volume. Weld solidification cracking in a 6061-T6 aluminum disk is studied in the second simulation (Dike et al. [1997]). Weld solidification cracking occurs as the material solidifies and is controlled by the material's cracking susceptibility and the loading conditions near the tail of the weld pool.

The thermal and mechanical analyses can be challenging due to difficulty in obtaining high temperature material property data. When data is available it is often less accurate at higher temperatures than at lower temperatures, and different sources of the same data are often not consistent. The material behavior can be very nonlinear which requires robust analysis codes and constitutive models as well as experienced analysts. Finally, supporting experimental work for material characterization and analysis validation are critical to any modeling effort.

PROCEDURES, RESULTS, AND DISCUSSION:

Thermal Analyses: Thermal finite element analyses were performed prior to mechanical analyses as the thermal and mechanical responses for the problems discussed here are not closely coupled. Temperature dependent thermal material properties were used for all analyses. The thermal conductivity was increased by approximately a factor of 4 above the melt temperature to account for enhanced heat transfer in the weld pool due to fluid motion. The latent heat of fusion was accounted for by modifying the specific heat as a function of temperature. Combined radiative and free convection heat losses were modeled. Temperature calculations were validated using weld fusion zone profiles and thermocouple data.

Mechanical Analyses: An internal state variable temperature and strain rate dependent constitutive model was used to model material behavior (Bammann et al. [1993]). The constitutive model is based on dislocation mechanics extended to a continuum framework with the evolution equations for the state variables placed in a hardening minus recovery format. The plasticity model is coupled with a ductile void growth damage model which acts to degrade the elastic moduli and concentrate the stress as damage accumulates. Failure occurs when the damage variable reaches a critical value. A parameter related to the rate of void growth is determined from notched tensile specimen tests. Temperature dependent elastic constants and thermal expansion data were used.

Weld Shrinkage in 304 L Stainless Steel Pipe: The specimens were 30.5 cm long, 7.6 cm outside diameter, and 0.9 cm thick. Three pass welds were made at the mid-length of the specimen in a modified U-shaped groove. Magnetic arc oscillation was used to achieve uniform filling of the groove during pipe rotation of 0.44 rpm. Instrumentation included thermocouples near the weld and LVDT's at two locations on one end of the pipe. The LVDT's were used to monitor axial displacement histories during welding at points +/- 90° from the weld torch position.

Figure 1 shows the axial motion of the two points on the free end of the pipe during welding. It was observed that agreement between analysis and experiment could be further improved by further decreasing the time step used in the

DISCLAIMER

mechanical analysis. The final axial shrinkage averaged around the weld circumference as measured between the ends of the pipe was 1.63 mm versus a calculated value of 1.52 mm.

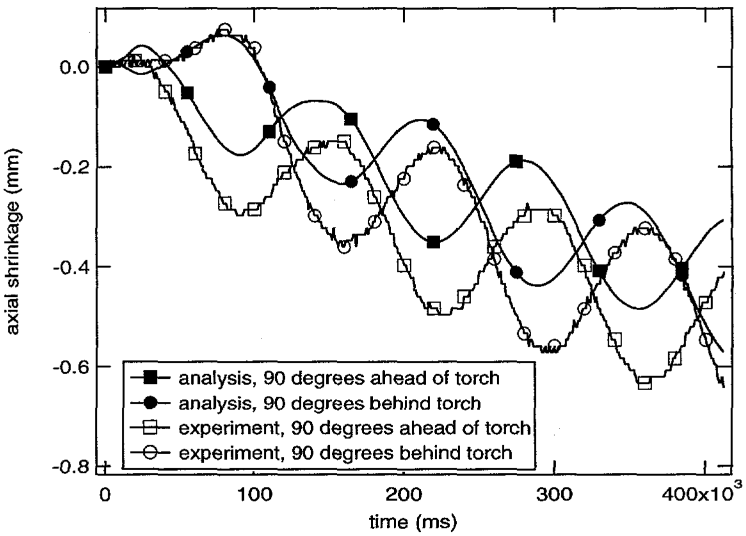

Figure 1. Axial motion of pipe end during welding.

Application to Weld Solidification Cracking: As solidification cracking occurs in a region of solidifying material, it is necessary to add additional detail to the model to account for solidification behavior and mechanical response at temperatures near the solidus temperature. For instance, it was necessary to use time steps small enough to accurately capture the solidification behavior. Near the liquidus temperature, the material solidifies very quickly, with nearly 70% solidified within 10° C of the liquidus temperature. Solidification is not complete, however, until the eutectic temperature is reached, nearly 100° C below the liquidus temperature. This very nonlinear rate of solidification can cause difficulties in the thermal analysis code. Time steps must also be small in the mechanical analysis in order to capture cracking that occurs by the time the material has been cooled to the solidus temperature. Temperature dependence of a parameter that controls the rate of void growth in the damage model was also included. Figure 2a shows an example of the observed cracking response for a 6.35 mm thick, 101 mm diameter 6061-T6 aluminum disk in which the weld is placed in a 13 mm wide groove. The current was increased at each 120° interval. In the experiment, a centerline crack formed at approximately 190° around the disk measured from the weld start, which then continued to follow the weld pool around the disk. Welds started at the top and proceeded clockwise. Figure 2b shows the calculated damage. The model shows cracks on both sides of the weld with the continuous crack beginning near 165° from the weld start. Incorporating information about the weld microstructure into the finite element analyses should improve the prediction of crack location relative to the weld centerline.

Figure 2. 6061-T6 aluminum disks with weld solidification cracks. (a) experiment, crack starts at 190° from weld start

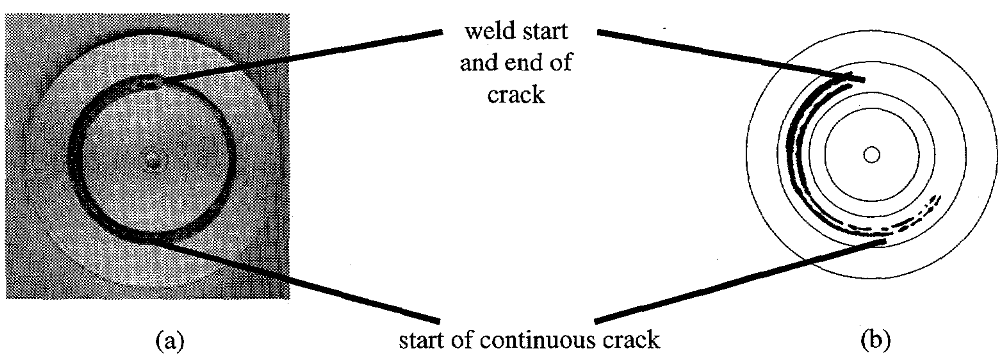

(which is top of figure), (b) finite element model, continuous crack starts near 165° from weld start. Dark areas represent failed elements (cracks).

Acknowledgment: This work was funded by the U.S. Department of Energy under contract No. DE-AC04-94AL85000.

REFERENCES:

1993 Bammann, D.J., Chiesa, M.L., Horstemeyer, M.F., and Weingarten, L.W., in Jones, N. and Wierzbicki, T. (eds.), Structural Crashworthiness and Failure, Elsevier Science Publishers, New York, pp. 1-54.

1997 Dike, J.J., Brooks, J.A., Bammann, D. J., and Li, M., Proc. ASM Int. European Conf. on Welding & Joining Science & Technology, Madrid, Spain, pp. 269-277.